

ORIGINAL RESEARCH

A novel role of breast cancer-derived hyaluronan on inducement of M2-like tumor-associated macrophages formation

Guoliang Zhang^{a,*}, Lin Guo^{b,*}, Cuixia Yang^a, Yiwen Liu^a, Yiqing He^a, Yan Du^a, Wenjuan Wang^a, and Feng Gao^c

^aDepartment of Molecular Biology, Shanghai Jiao Tong University Affiliated Sixth People's Hospital, Shanghai, P. R. China; ^bDepartment of clinical Laboratory, Shanghai Oncology Hospital, Shanghai Fudan University School of Medicine, Shanghai, P. R. China; ^cDepartment of Molecular Biology and Clinical Laboratory, Shanghai Jiao Tong University Affiliated Sixth People's Hospital, Shanghai, P. R. China

ABSTRACT

Microenvironmental signals determine the differentiation types and distinct functions of macrophages. Tumor-associated macrophages (TAM) constitute major infiltrates around solid tumor cells and accelerate tumor progression due to their immunosuppressive functions. However, the mechanisms through which tumor microenvironment modulates macrophages transition are not completely elucidated. Hyaluronan (HA), a prominent component in tumor microenvironment, is a notable immunoregulator and its high level is often related to poor prognosis. Herein, we found that the number of M2 macrophages was highly correlated with HA expression in tumor tissues from breast cancer patients. Experimental data showed that breast cancer-derived HA stimulated M2-like TAM formation in a mouse model and had multiple effects on macrophages transformation *in vitro*, including upregulating CD204, CD206, IL-10 and TGF- β , activating STAT3 signal, and suppressing killing capacity. These data indicate that HA derived from breast cancer activates macrophages in an alternative manner. Further mechanism study revealed that HA-CD44-ERK1/2-STAT3 pathway served as an important regulator in M2-like TAM formation. Therefore, targeting TAM by abrogating HA-CD44 interaction may be a potential strategy for breast cancer immunotherapy.

ARTICLE HISTORY

Received 18 December 2015
Revised 18 March 2016
Accepted 24 March 2016

KEYWORDS

Breast cancer; CD44; ERK1/2; hyaluronan; STAT3; tumor-associated macrophages

Introduction


Macrophages originate from monocytic precursors in the blood and transform into specialized phenotypes depending on local conditions in tissues. In response to various signals, macrophages may undergo classical M1 activation (stimulated by bacterial products or IFN γ) or alternative M2 activation (stimulated by IL-4/IL-13).¹ Important features of M1 macrophages include the expression of pro-inflammatory cytokines, promotion of Th1 response, and strong microbicidal and tumoricidal activity. In contrast, M2 macrophages are characterized by high expression of scavenger and mannose receptors, release of anti-inflammatory molecules, modulation of tissue remodeling, and downregulation of inflammation.² Macrophages comprise the dominant portion of leukocyte population within the tumor microenvironment, and tumor-associated macrophages (TAM) have been identified as immunosuppressive M2-like phenotype.²⁻⁵ M2-polarized TAM promote tumor growth by stimulating angiogenesis, secreting growth factors, suppressing immune responses, or facilitating invasion and metastasis. In breast carcinomas, TAM density correlates with poor prognosis, and eliminating macrophages from the tumor site, either via genetic or therapeutic means, leads to retarded tumor progression.^{4,6}

As TAM have important clinical significances, it is necessary to explore the precise mechanisms regarding TAM polarization. It is generally assumed that tumor microenvironment is a critical determinant of the phenotype of local macrophages.

Recent studies have reported that M-CSF, heat shock protein 27 (Hsp27), TGF- β , sphingosine-1-phosphate (S1P) secreted by breast cancer cells, and IL-4 released by tumor-infiltrating lymphocytes may influence the TAM transition.⁷⁻¹⁰ As breast tumor microenvironment contains both cellular and non-cellular (matrix) compositions, the currently reported molecules cannot fully explain the role of breast tumor microenvironment in the formation of TAM with M2 phenotype. Hyaluronan (HA), a major component of extracellular matrix (ECM), is one of the most abundant molecules within most malignant tumor microenvironments. As an unbranched polymer composed of repeating glucuronic acid and N-acetyl glucosamine disaccharide units, HA is accumulated both in the pericellular milieu surrounding tumor cells and in the tumor stroma.¹¹ Clinical and experimental data indicate that HA abnormally accumulates in breast cancer compared to normal breast epithelium, and correlates to poor prognosis.^{12,13} Moreover, as an important immunoregulator, HA has the ability to regulate immunoactivities of macrophages, such as stimulating chemokine production of macrophages in acute lung injury.¹⁴ All the above findings suggest that HA derived from breast cancer cells may serve as a crucial player in the formation of M2-like TAM within breast tumor microenvironment. Besides HA, the major HA receptor CD44 is also activated and highly expressed on macrophages during tumor microenvironment remodeling.¹⁵

CONTACT Feng Gao  gao3507@126.com

*G. Zhang and L. Guo contributed equally to this work.

 Supplemental data for this article can be accessed on the [publisher's website](#).

Additional reports indicate that tumor cells can deactivate monocytes via CD44.^{16,17} With supporting data from other laboratories and ours showing that CD44 participates in cell differentiation,^{18,19} it seems that HA-CD44 axis may act together in TAM-polarizing formation.

In this study, we attempted to investigate the potential of breast cancer-derived HA in the inducement of M2-like TAM. We first analyzed the HA expression levels and the amount of M2 macrophages accumulated in human breast cancer and benign tissues. Then, we investigated the effects of HA derived from breast cancer cells on macrophage phenotype transition *in vitro* by using human peripheral blood monocytes and human monocytic cell line THP-1 as studying models.²⁰ Furthermore, an *in vivo* experiment was conducted in a mouse model to verify the role of breast cancer-derived HA. Finally, we tried to reveal the underlying mechanisms by studying HA-CD44-ERK1/2-STAT3 signal pathway. Our results showed that breast cancer-derived HA-induced M2 polarization of macrophages through interacting with CD44 and activating ERK1/2-STAT3 pathway.

Results

The amount of M2 macrophages is correlated with HA expression in human breast malignant tissues

Previous reports have proved that HA accumulates in breast cancer tissues and correlates to poor prognosis.^{12,13} To determine whether HA-enriched breast tumor microenvironment is associated with the formation of TAM with M2 phenotype, immunohistochemistry was applied to analyze the HA expression and the number of M2 macrophages on serial sections of tissues derived from patients diagnosed with breast cancer or benign diseases. CD204 and CD206 were used as specific markers of M2 macrophages as previously described.^{21,22} As shown in Fig. 1A, HA content was low in human breast benign tissues where CD204⁺ or CD206⁺ macrophages were also hardly detected. In contrast, intense HA staining was observed in human breast cancer tissues and mainly distributed around cancer cell islets. In accordance with HA deposition, considerable CD204⁺ or CD206⁺ macrophages were located within or near the stroma surrounding cancer cell islets. Statistical analysis showed that the levels of HA, CD204⁺ macrophages, and CD206⁺ macrophages between benign and malignant tissues were significantly different (Figs. 1B–D). In order to further understand their clinical values, we examined the relationship among HA expression level, M2-like TAM number, and clinicopathologic characteristics. As shown in Table 1, the elevated HA intensity and the increase of CD204⁺/CD206⁺ macrophages were both related to tumor size, lymph node positivity, and poor tumor differentiation. Moreover, the correlation analysis revealed that HA expression was positively correlated with the amount of CD204⁺ or CD206⁺ macrophages in human breast malignant tissues (Figs. 1E and F). Together, these results suggest that the abnormal accumulation of HA in breast tumor microenvironment contributes to M2 polarization in macrophages.

Inducement of M2 macrophages by breast cancer cells with different HA expression levels

To verify our hypothesis, two breast cancer cell lines with either high or low HA expressing potential were selected. The capacities of breast cancer cells to induce M2 macrophages formation were assessed by using human peripheral blood monocytes and human monocytic cell line THP-1 as studying models.²⁰ First, as described before, we used PMA/IL-4/IL-13 and IL-4/IL-13 as positive controls to induce THP-1 cells and monocytes, respectively. As expected, THP-1 cells differentiated to macrophages with significant expression of cell surface markers for M2 macrophages, including CD14, CD204, and CD206 (Fig. 2A). Monocytes isolated from peripheral blood of healthy donors also transited to CD204- or CD206-positive macrophages (Fig. 2A). When monocytes develop into TAM, the signal transducer and activator of transcription 3 (STAT3) could be phosphorylated and associated with TAM bioactivities, such as secreting cytokines that accelerate tumor malignancy.²³ Our data showed that STAT3 phosphorylation levels in THP-1 cells and monocytes were remarkably increased when stimulated with PMA/IL-4/IL-13 or IL-4/IL-13 (Fig. 2B). The above results indicated that THP-1 cells and monocytes have the ability to polarize to M2 macrophages after treatment with corresponding cytokines. To investigate whether breast cancer-derived HA contributes to monocytes transformation as well, human breast cancer cells BT-549 (HA^{high}) and MCF-7 (HA^{low}) were applied for the inducement (Figs. S1A, C, D, F). After co-cultured with BT-549 cells, THP-1 cells presented high expression of CD14/CD204/CD206 and enhanced phosphorylation of STAT3. When exposed to BT-549 supernatant containing high level of HA, peripheral blood-derived monocytes also exhibited increased STAT3 phosphorylation and a markedly altered phenotype, with elevated expression of CD204/CD206 and retained CD14 molecules. In contrast, MCF-7 cells and MCF-7 supernatant showed no significant effects on phenotype conversion of THP-1 cells and monocytes. (Figs. 2A and B). As the immunosuppressive macrophages, TAM suppress immunological responses through secreting many anti-inflammatory cytokines in which IL-10 and TGF- β are most important.^{24–26} Next, we determined whether breast cancer-derived HA affects the bioactivities of macrophages by measuring the secretion levels of IL-10 and TGF- β . The ELISA assay showed that IL-4/IL-13 (positive control) and BT-549 supernatant facilitated monocytes to release IL-10 and TGF- β , whereas MCF-7 supernatant had no significant effect (Figs. 2C and D). In addition, different from M1 macrophages, TAM lose the capacity to kill cancer cells. To confirm that the phenotype conversion induced by HA^{high} breast cancer cells could influence the following effects of macrophages on cancer cells, a cytotoxicity assay was performed. The data indicated that monocytes pre-exposed to BT-549 supernatant showed considerably decreased capacity to induce the apoptosis of cancer cells when compared with control monocytes (Fig. 2E), suggesting that macrophages lose the killing potential in the presence of high level of HA. Collectively, these results demonstrate that breast cancer cells

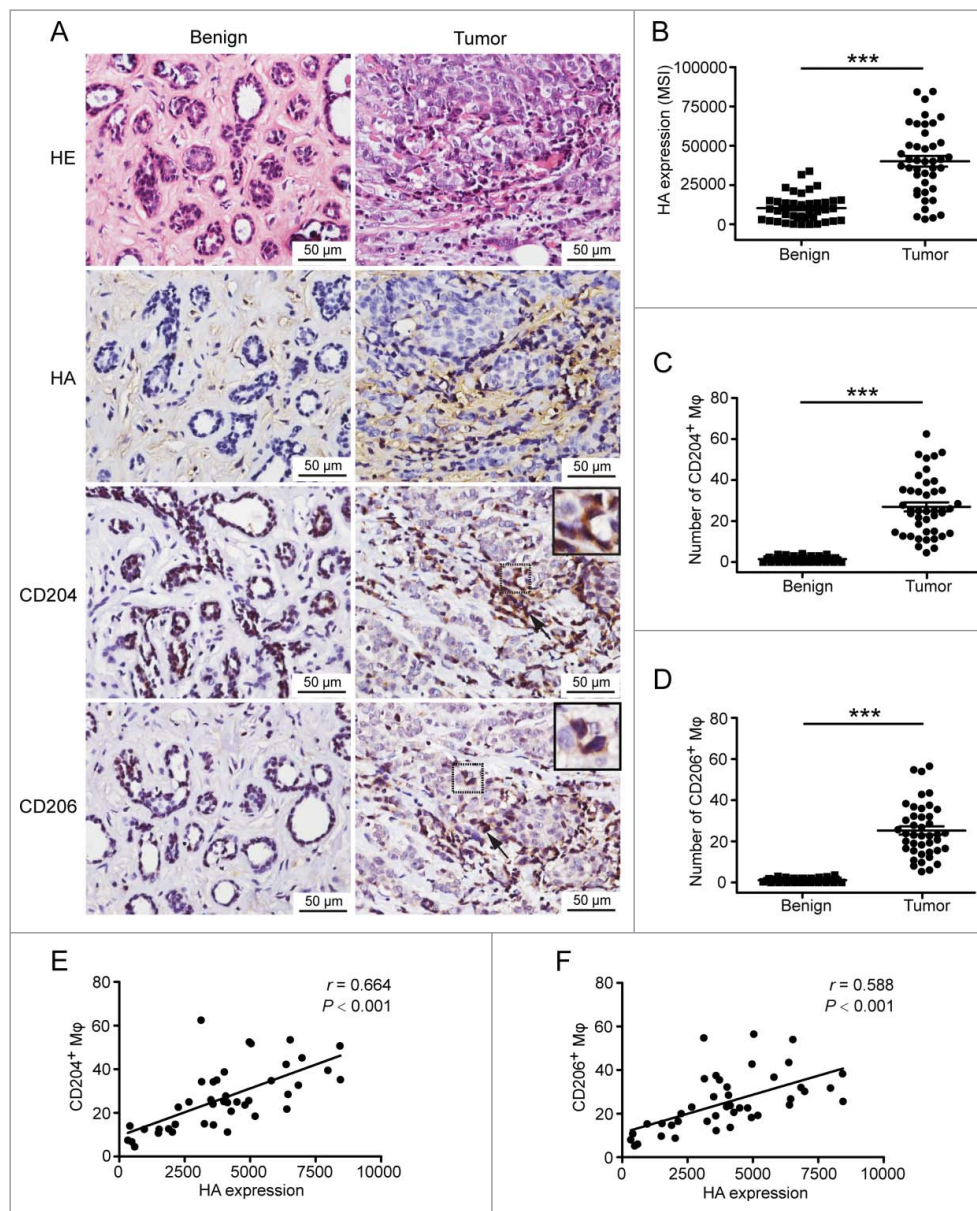


Figure 1. The amount of M2 macrophages is correlated with HA expression in human breast malignant tissues. (A) Immunohistochemical analysis showing HE staining, HA content, CD204⁺ macrophages, and CD206⁺ macrophages in human breast benign and malignant tissues. Shown are representative images from 40 patients with breast benign diseases and 42 breast cancer patients. (B–D) Scatter plots showing levels of HA (B), CD204⁺ macrophages (C), and CD206⁺ macrophages (D) in tissue samples of patients with breast cancer (n = 42) and benign diseases (n = 40). *** $p < 0.001$ by Student's t-test. (E, F) Scatter plots showing the positive correlation between HA expression and the number of CD204⁺/CD206⁺ macrophages in tissue samples of breast cancer patients (n = 42). Pearson's coefficient tests were performed to assess statistical significance.

with high HA expression educate monocytes to converse to macrophages with M2-like phenotypes and functions.

4-MU inhibits the formation of M2 macrophages by suppressing HA synthesis

To identify whether HA is the pivotal mediator in TAM polarization, 4-Methylumbelliferone (4-MU), the HA synthesis inhibitor, was administrated to suppress HA biosynthesis in BT-549 cells. The concentration of 4-MU was set at 500 μmol/L that had no cytotoxic effect on BT-549 cells (Fig. S1B). After treatment with 4-MU, HA production was reduced by nearly 65% (Fig. S1C). As a result, the transformation of THP-1 cells and monocytes was inhibited (Fig. 3).

In particular, the capacity of 4-MU treated BT-549 cells to induce CD14/CD204/CD206 expression and STAT3 signal activation in THP-1 cells was significantly lower than that of BT-549 cells without 4-MU addition (Figs. 3A and B). Similarly, the levels of CD204/CD206 expression and STAT3 phosphorylation were dramatically decreased in monocytes incubated with supernatant of 4-MU treated BT-549 cells (Figs. 3A and B). Furthermore, when exposed to supernatant of BT-549 cells treated with 4-MU, the levels of IL-10 and TGF-β secreted by monocytes were also decreased, whereas the cytotoxicity of monocytes was increased significantly (Figs. 3C–E). The data suggest that HA derived from breast cancer cells is responsible for the formation of M2 macrophages.

Table 1. Clinicopathologic characteristics of study population in relation to HA expression, CD204⁺ macrophages, and CD206⁺ macrophages.

Clinicopathologic parameter	n	HA expression (IOD)			CD204 ⁺ macrophages			CD206 ⁺ macrophages		
		Median	95% CI	<i>p</i>	Median	95% CI	<i>p</i>	Median	95% CI	<i>p</i>
Age										
<50 y	12	43,940	27,864–5,9465	0.509	25.25	19.12–39.17	0.421	22.96	17.06–35.42	0.756
≥50 y	30	38,632	30,875–46,433		24.75	20.07–30.34		23.38	20.13–29.54	
Tumor size										
<2 cm	16	31,935	17,677–43,358	0.024*	14.25	12.88–28.81	0.032*	15.40	13.21–26.89	0.043*
≥2 cm	26	42,023	38,495–53,369		25.50	25.31–35.92		23.88	23.38–32.55	
Histologic type										
Invasive duct	26	39,993	34,271–50,564	0.385	26.88	24.25–34.61	0.150	26.21	23.13–33.34	0.056
Others	16	38,126	23,199–49,394		16.75	14.17–31.44		17.38	13.75–26.98	
Histologic grade										
1	8	26,909	9,125–39,615	0.025*	11.25	4.900–23.29	0.007*	13.67	5.349–25.37	0.024*
2	17	37,905	27,617–48,935		25.25	19.80–33.09		22.84	18.59–30.67	
3	17	42,718	40,138–61,194		35.00	26.32–40.66		29.38	24.29–37.61	
Lymphnode metastasis										
Yes	12	45,817	39,807–62,023	0.043*	34.67	27.58–38.59	0.030*	32.00	25.02–38.09	0.045*
No	30	37,905	27,628–44,221		22.18	18.74–30.31		19.96	17.76–27.65	
ER										
Negative	17	42,718	33,053–58,388	0.172	25.00	20.57–34.77	0.782	23.75	19.43–31.00	0.994
Positive	25	35,909	28,277–44,267		25.00	20.19–32.59		20.00	19.35–31.14	
PR										
Negative	24	40,706	33,545–52,815	0.295	24.38	21.14–32.96	0.945	23.21	19.99–30.48	0.999
Positive	18	38,541	25,803–46,117		25.46	19.13–34.33		23.25	18.23–32.24	
HER2										
Negative	19	40,625	26,904–49,870	0.653	25.00	17.81–32.30	0.455	22.67	16.91–30.51	0.485
Positive	23	37,180	32,605–50,373		25.00	22.40–34.47		23.25	21.34–31.77	
Ki67										
<20%	20	38,557	30,177–50,482	0.918	24.34	19.07–33.28	0.737	22.84	18.58–31.01	0.838
≥20%	22	39,993	29,681–49,593		25.13	21.39–33.75		23.50	19.86–31.41	

*Indicated statistical significance ($p < 0.05$)

Over-expression of HA promotes M2 macrophages formation *in vitro* and *in vivo*

As shown in Fig. 2, MCF-7 cells had no significant effect on M2 macrophages formation due to the low expression of HA. To further confirm the role of HA derived from breast cancer cells in phenotype conversion of macrophages, we transfected MCF-7 cells with HA synthase 2 (HAS2) and established a stable MCF-7 cell line over-expressing HA, named MCF-7^{HAS2} (Figs. S1D–F). Compared with parental and mock-transfected cells, MCF-7^{HAS2} cells and supernatant significantly increased the levels of CD204/CD206 expression and STAT3 phosphorylation in THP-1 cells and monocytes, respectively (Figs. 4A and B). In addition, when stimulated with MCF-7^{HAS2} supernatant, the levels of IL-10 and TGF- β secreted by monocytes were enhanced as well (Figs. 4C and D). To further verify the potential of HA, 4-MU was added to suppress HA synthesis in MCF-7^{HAS2} cells. As expected, the phenotype transformation of monocytes induced by MCF-7^{HAS2} cells was inhibited (Fig. S2). These results prove that HA derived from breast cancer cells drives the transformation of monocytes to M2 macrophages. To define the contribution of HA in TAM polarization *in vivo*, MCF-7^{mock} and MCF-7^{HAS2} cells were implanted into the mammary fat pads of NOD/SCID mice, and the tumors were isolated for immunohistochemistry assay. The histological evaluation showed that the HA expression level and the number of CD204⁺/CD206⁺ macrophages were significantly higher in tumors formed by MCF-7^{HAS2} cells than that in tumors induced by MCF-7^{mock} cells (Fig. 5), further clarifying the critical role of breast cancer-derived HA in M2-like TAM formation.

Involvement of HA-CD44 interaction in the formation of M2 macrophages

CD44 is the major cell surface receptor for HA. To determine whether breast cancer-derived HA induces M2-like TAM formation through binding to CD44, the blockage experiment was conducted. Pretreatment of THP-1 cells with anti-CD44 mAb (IM7)²⁷ effectively inhibited the expression of CD14/CD204/CD206 and the phosphorylation of STAT3 mediated by BT-549 cells (Figs. 6A and B). Similarly, blocking of CD44 suppressed CD204/CD206 expression and STAT3 phosphorylation in monocytes stimulated by BT-549 supernatant (Figs. 6A and B). In addition, the elevated secretion of IL-10/TGF- β and the decreased cytotoxicity of monocytes induced by BT-549 supernatant were inhibited by adding the anti-CD44 mAb (Figs. 6C–E). The isotype IgG had no effects in all corresponding experiments. The results indicate that cell membrane CD44 is responsible for the HA-induced M2 polarization of macrophages.

ERK1/2-STAT3 pathway is involved in macrophages transformation

To further understand the intracellular mechanism after the binding of HA to CD44 on macrophages, we next studied one of the important cellular signal pathways, ERK1/2, which has been regarded as a crucial regulator of cell differentiation and reported to interact with CD44 directly.^{28,29} The western blot analysis showed that ERK1/2 phosphorylation in THP-1 cells and monocytes were considerably elevated after exposed to BT-

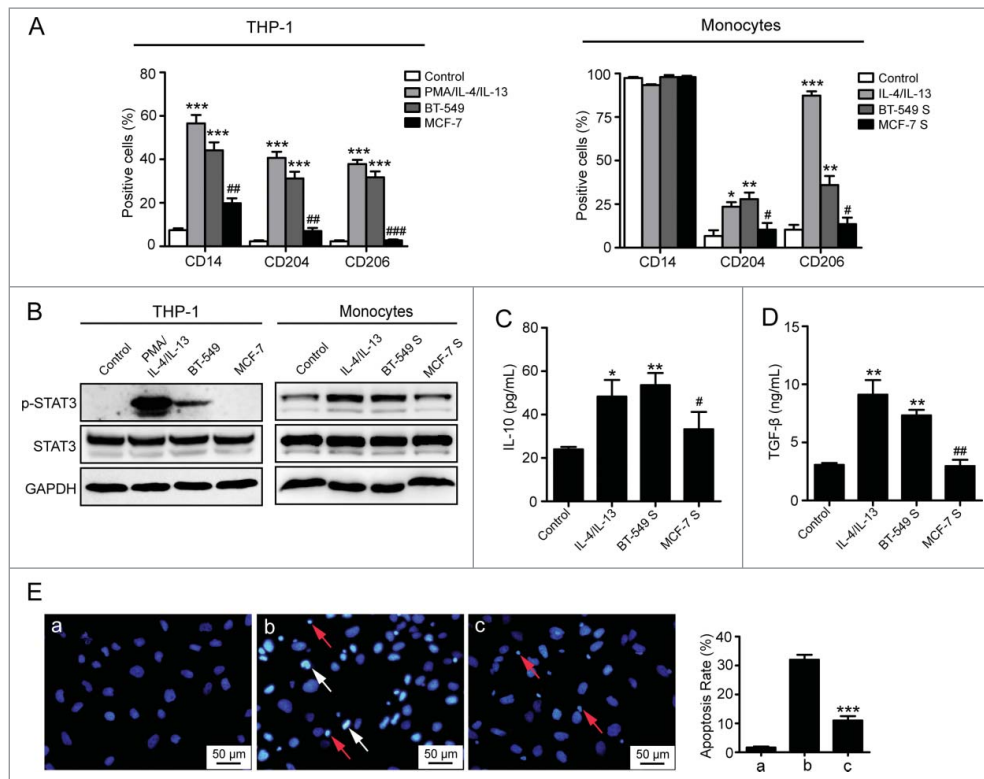


Figure 2. Inducement of M2-like macrophages by breast cancer cell lines with different HA expression levels. (A) Flow cytometry analysis showing expression levels of CD14, CD204, and CD206 in THP-1 cells and monocytes. (B) Western blot analysis of STAT3 phosphorylation levels of THP-1 cells and monocytes. (C, D) Levels of IL-10 and TGF- β secreted by monocytes were measured by ELISA assay. (E) Apoptosis of BT-549 cells induced by monocytes. (a) BT-549 cells cultured in normal condition; (b) BT-549 cells co-cultured with monocytes which were cultured in normal medium for 72 h; (c) BT-549 cells co-cultured with monocytes which were pretreated with 50% BT-549 supernatant for 72 h. The ratio of apoptotic BT-549 cells was determined by manually counting white condensed pyknotic nuclei (white arrows point to the representative apoptotic nuclei of BT-549 cells, and red arrows point to the nuclei of monocytes). At least five fields were counted for each experimental group. Data represented are shown as mean \pm s.d. from three independent experiments. * p < 0.05, ** p < 0.01, *** p < 0.001 (* VS Control); # p < 0.05, ## p < 0.01, ### p < 0.001 (# VS BT-549 or BT-549S).

549 cells and the supernatant, respectively (Fig. 7A). Also, the increase was inhibited by 4-MU-induced suppression of HA synthesis (Fig. 7A), suggesting that HA derived from breast

cancer cells activated ERK1/2 signal during the conversion of monocytes. To further identify the role of ERK1/2 signal, a MAPK kinase inhibitor, U0126, was administered. The results

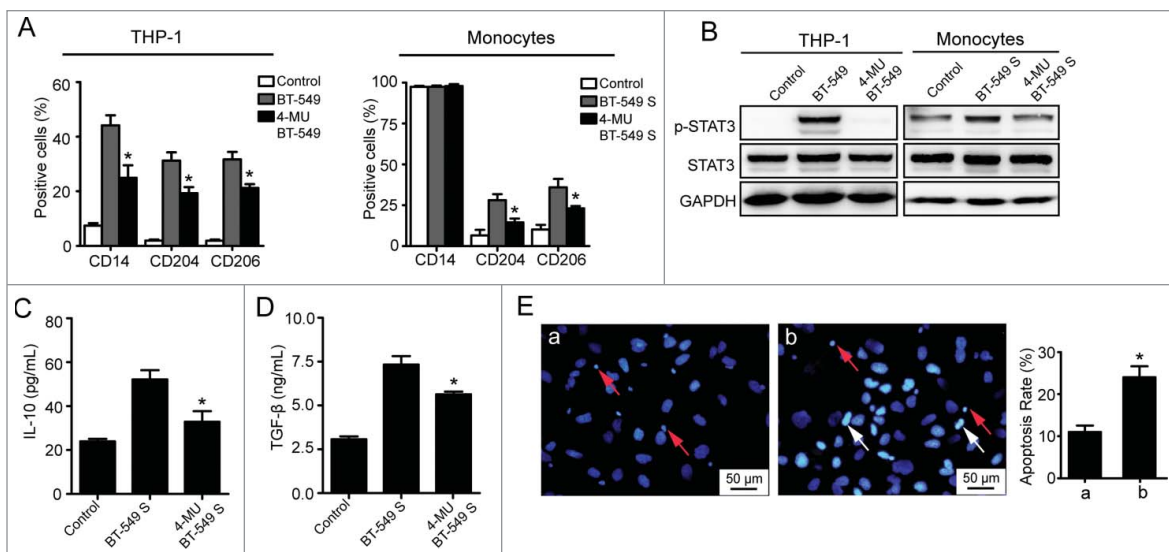


Figure 3. 4-MU inhibits the formation of M2 macrophages by suppressing HA synthesis. (A) Flow cytometry analysis showing expression levels of CD14, CD204, and CD206 in THP-1 cells and monocytes. (B) Western blot analysis of STAT3 phosphorylation levels of THP-1 cells and monocytes. (C, D) Levels of IL-10 and TGF- β secreted by monocytes were measured by ELISA assay. (E) Apoptosis of BT-549 cells induced by monocytes. (a) BT-549 cells co-cultured with monocytes which were treated with 50% BT-549 supernatant for 72 h. (b) BT-549 cells co-cultured with monocytes which were cultured in 50% supernatant of 4-MU treated BT-549 cells for 72 h. All data represented are shown as mean \pm s.d. from three independent experiments. * p < 0.05, ** p < 0.01, *** p < 0.001 (* VS BT-549 or BT-549S).

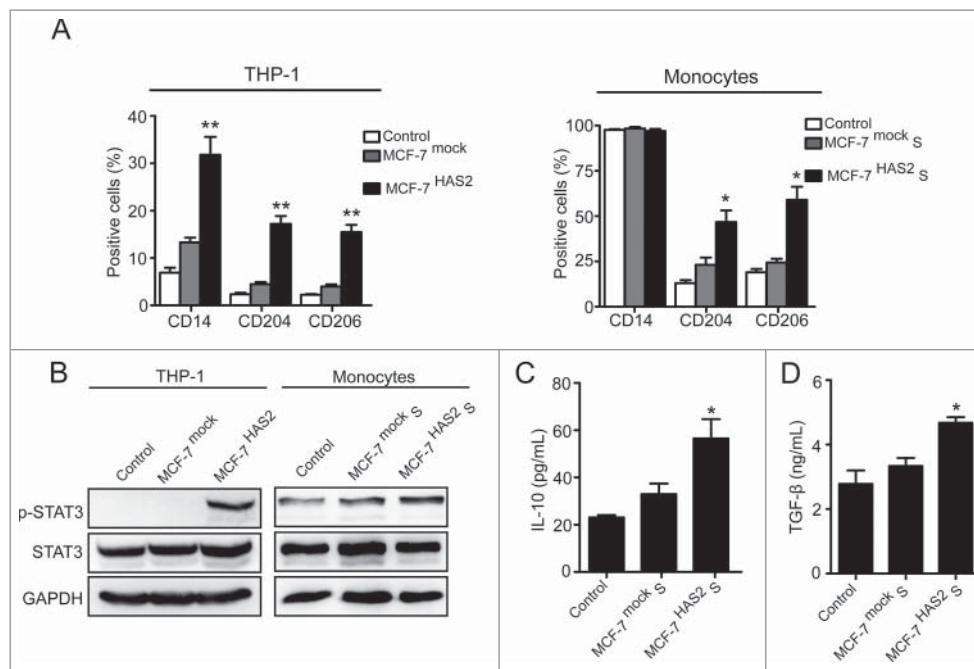


Figure 4. Over-expression of HA promotes M2 macrophages formation. (A) Flow cytometry analysis showing expression levels of CD14, CD204, and CD206 in THP-1 cells and monocytes. (B) Western blot analysis of STAT3 phosphorylation levels of THP-1 cells and monocytes. (C, D) Levels of IL-10 and TGF- β secreted by monocytes were measured by ELISA assay. Graphs represent the mean \pm s.d. from three independent experiments. * $p < 0.05$, ** $p < 0.01$, *** $p < 0.001$ (* VS MCF-7^{mock} S or MCF-7^{mock} S).

showed that ERK1/2 phosphorylation induced by BT-549 cells and supernatant was significantly decreased in the presence of U0126 (Fig. 7A). Meanwhile, U0126 also inhibited the transformation of THP-1 cells and monocytes (Figs. 7B–E), indicating that ERK1/2 signal activated by HA derived from breast cancer cells participated in monocytes transformation. As described previously, the phosphorylation level of STAT3 was elevated by HA derived from breast cancer cells (Fig. 3B), suggesting that STAT3 signal is involved in TAM formation. To prove this, a STAT3 inhibitor, S3I-201,^{30,31} was administrated to human peripheral blood monocytes. The results demonstrated that STAT3 phosphorylation and phenotype conversion of monocytes induced by BT-549 supernatant were simultaneously suppressed by S3I-201 (Figs. 7F–I), confirming the important role of STAT3 in monocytes transformation. Given that STAT3 phosphorylation of monocytes was also inhibited by U0126 (Fig. 7C), we proposed that ERK1/2-STAT3 pathway was critical during TAM formation. In addition, blocking of CD44 on THP-1 cells or monocytes suppressed ERK1/2 and STAT3 phosphorylation mediated by BT-549 cells or supernatant (Figs. 6B and 7A), suggesting that breast cancer cell-derived HA activated ERK1/2-STAT3 signal pathway through interacting with CD44. These results, together with the data shown in Fig. 6, demonstrate that CD44-ERK1/2-STAT3 pathway is the main effector in M2-like TAM formation induced by breast cancer-derived HA.

Discussion

TAM accumulated in breast tumor are polarized M2 cells that suppress antitumor immunity and promote cancer progression.^{3,4} Although a few tumor microenvironment-derived cytokines have been demonstrated to regulate the plasticity of TAM phenotypes and functions,^{7–10} the current reports cannot fully

explain how M2-like TAM form. ECM is extensively remodeled in tumor microenvironment and its active products have been reported to regulate immunoresponses.³² HA, the most abundant component of ECM, acts as both a pro- and anti-inflammatory molecule *in vivo*. For example, HA is identified to induce potent pro-inflammatory responses in macrophages during lung injury and repair.¹⁴ As HA is abnormally increased in breast cancer and related to poor prognosis, it is reasonable to assume that HA may contribute to TAM polarization through mediating anti-inflammatory responses in macrophages within breast tumor microenvironment.

In this study, we found that HA was highly expressed in breast cancer tissues of patients, which is consistent with previous reports.¹² Meanwhile, the amount of M2-like TAM (CD204 or CD206 positive) were also increased and mainly distributed at the sites of HA deposition. Notably, the statistical analysis indicated that HA expression was positively correlated with the number of M2-like TAM. This is supported by a recent pathological study that displayed a fascinating link between HA accumulation and high numbers of macrophages, especially M2-like (CD163 positive).³³ Moreover, in accordance with prior studies, our clinical analysis demonstrated that both HA and M2-like TAM were related to the malignancy of breast cancer, such as tumor size, histologic grade, and lymph node metastasis. Based on these, we believe that HA and TAM may accelerate breast cancer development together through interacting with each other that is not completely elucidated. It has been shown that HA has the capacity to recruit macrophages into breast tumor stroma,³⁴ whereas our results indicated that macrophages surrounded by HA in breast cancer showed M2 polarized feature. These findings prompt us to ask how macrophages recruited by HA converse to M2-like TAM in breast tumor microenvironment. In order to understand this transformation process, we explored the potential of HA in TAM

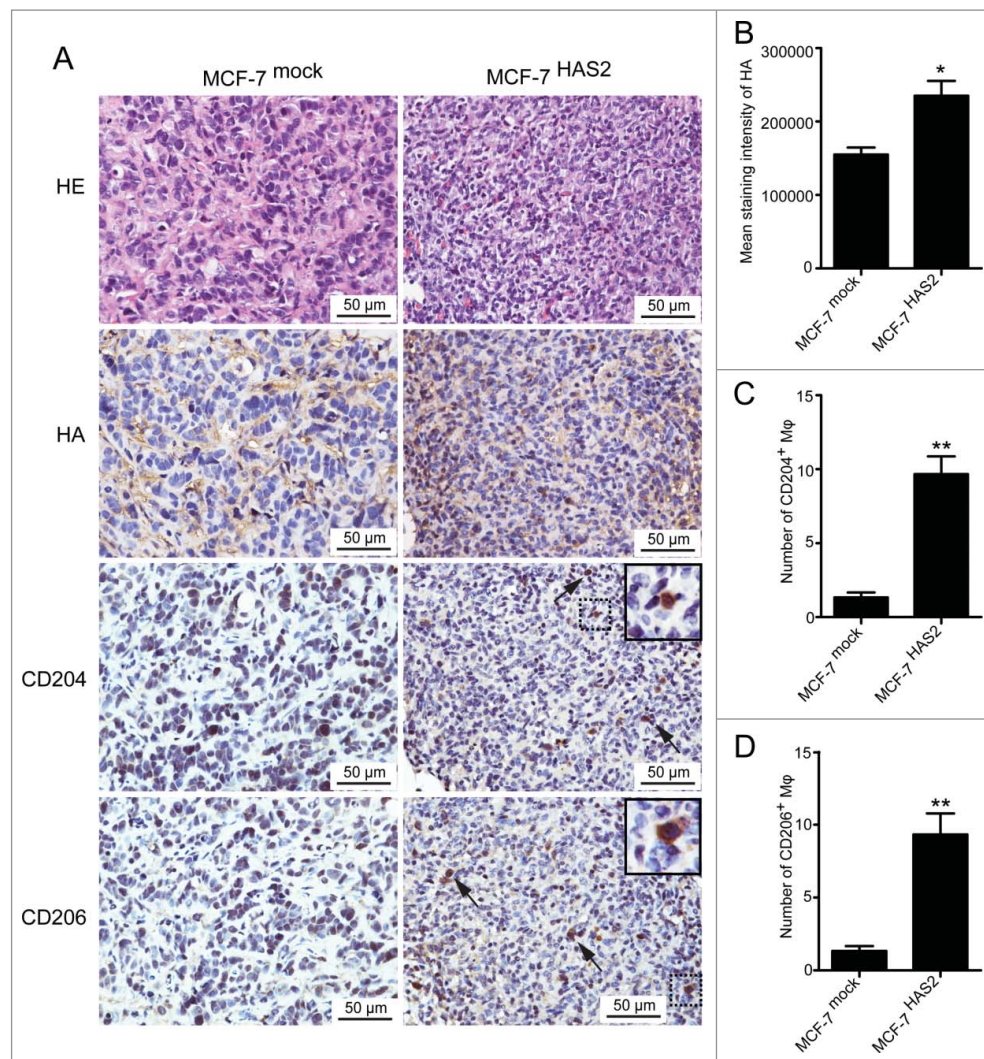


Figure 5. HA over-expressed breast cancer cells induce M2 macrophages formation *in vivo*. (A) Immunohistochemical analysis showing HE staining, HA expression, CD204⁺ macrophages, and CD206⁺ macrophages in tissue samples of mouse breast tumors formed by MCF-7^{mock} cells or MCF-7^{HAS2} cells. (B–D) Box plots showing levels of HA, CD204⁺ macrophages, and CD206⁺ macrophages in tissue samples of tumors formed by MCF-7^{mock} cells (n = 3) and MCF-7^{HAS2} cells (n = 3). Data represented are shown as mean ± s.d. *p < 0.05, **p < 0.01.

polarization. We first investigated whether HA derived from breast cancer cells affects phenotype transition of macrophages. Specific markers for M2 macrophages were analyzed to evaluate macrophage phenotypes, including CD204, CD206, STAT3, IL-10, and TGF- β .^{21-24,35} Our data showed that breast cancer cells BT-549 (HA high expressing), but not MCF-7 (HA low expressing), significantly induced monocytes developing into macrophages with M2 phenotype, suggesting that HA is involved in this process. As breast cancer cells secrete numerous molecules, the above result cannot exclude the role of other factors that may contribute to macrophages activation. To determine whether this cell type transition is primarily initiated by HA, 4-MU, the well-known HA synthesis inhibitor, was administrated to suppress HA biosynthesis in BT-549 cells. Given that 4-MU at high concentration may have cytotoxic effect on cells,³⁶ we priorly evaluated its cytotoxicity and took a concentration that extremely inhibited HA synthesis without affecting BT-549 cells proliferation. We found that 4-MU repressed M2 macrophages formation mediated by BT-549 cells, suggesting that breast cancer-derived HA promotes monocytes transforming to M2-like TAM. The result was also

supported by other findings that HA derived from cervical, hepatoma, glioma, and lung carcinoma cells could induce formation of immunosuppressive macrophages *in vitro*.²⁴ However, a few recent studies point out that 4-MU may influence the synthesis of other glycosaminoglycans, such as chondroitin sulfate, heparin sulfate, and decorin.^{37,38} To exclude their possible effects on monocytes differentiation, we over-expressed HA in MCF-7 cells to investigate its role in macrophages activation for a further confirmation. Three isoforms of HA synthase (HAS) have been identified in humans, in which HAS2 is essential for initiation and progression of breast cancer and its products are documented to have immunoregulating functions.^{24,39} More importantly, it is reported that 4-MU-induced inhibition of HA in mammary tumor cells is mainly attributed to HAS2 repression.⁴⁰ Therefore, we transfected MCF-7 cells with HAS2 and found that MCF-7^{HAS2} cells markedly induced macrophages phenotype transformation due to elevated HA expression. Moreover, as expected, the MCF-7^{HAS2} cells-mediated macrophages activation was blocked by 4-MU as well, demonstrating that HA synthesized by HAS2 is responsible for M2-like TAM formation. These findings, together with our

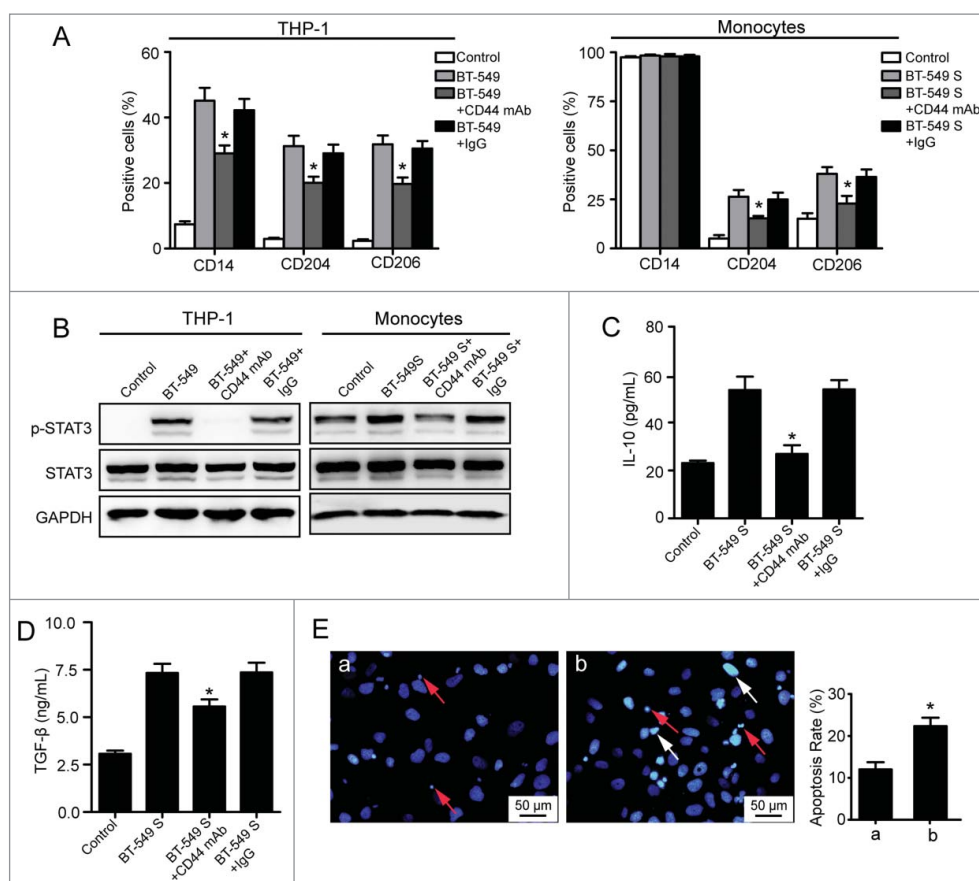


Figure 6. Involvement of HA-CD44 interaction in the formation of M2 macrophages. (A) Flow cytometry analysis showing expression levels of CD14, CD204, and CD206 in THP-1 cells and monocytes. (B) Western blot analysis of STAT3 phosphorylation levels of THP-1 cells and monocytes. (C, D) Levels of IL-10 and TGF- β secreted by monocytes were measured by ELISA assay. Graphs represent the mean \pm s.d. from three independent experiments. (E) Apoptosis of BT-549 cells induced by monocytes. (a) BT-549 cells co-cultured with monocytes which were pretreated with non-immune IgG (10 μ g/mL) and cultured in 50% BT-549 supernatant for 72 h. (b) BT-549 cells co-cultured with monocytes which were pretreated with anti-CD44 mAb (10 μ g/mL) and cultured in 50% BT-549 supernatant for 72 h. The data represented are shown as mean \pm s.d. from three independent experiments. * p < 0.05 (* VS BT-549+IgG or BT-549S+IgG).

clinical data, strongly suggest that HA derived from breast cancer induces TAM polarization, which in turn may accelerate breast cancer progression.

It is well accepted that the crosstalk between macrophages and tumor cells is a fundamental step in driving breast cancer malignancy. When TAM transit to M2 phenotype, they become facilitative to cancer progression. However, apart from phenotype alterations induced by different factors, the following effects of changed macrophages on cancer cells were not usually observed in previous relevant studies, including the cytotoxicity of macrophages.^{24,41} In this study, we not only confirmed the potential of HA in affecting phenotype conversion of macrophages, but also determined the influence of HA on macrophages killing capacity. When pre-treated with BT-549 supernatant containing high amount of HA, the killing potential of macrophages was effectively inhibited, which could be abrogated by suppressing HA synthesis. As losing the ability to kill cancer cells is one of the prominent characteristics of TAM, our data further imply that HA contributes to the formation of immunosuppressive TAM, partially explaining why breast cancer with abundant HA could escape from immunotoxicity and progress rapidly.^{12,33} As *in vitro* experiments cannot completely mimic the *in vivo* environment, to further confirm our results, an animal model was conducted by implanting MCF-7^{mock} cells

(low HA expressing) and MCF-7^{HAS2} cells (high HA expressing) into the mammary fat pads of NOD/SCID mice. In contrast to breast tumors formed by MCF-7^{mock} cells, the MCF-7^{HAS2} cells-induced tumors significantly harbored more M2-like TAM. These data are consistent with our clinical results obtained from breast cancer patients, further verifying the critical role of HA in TAM polarization.

Given that HA is the key factor that mediates TAM formation within breast tumor microenvironment, it is necessary to uncover the following mechanisms in terms of finding a target for breast cancer immunotherapy. As proved before, CD44 is the major cell surface receptor for HA and HA-CD44 axis appears to be increasingly significant in regulating immunological responses, such as mature B cells activation, T cells recruitment, and monocytes deactivation.⁴² We found that antagonizing the HA-CD44 interaction between breast cancer cells and monocytes significantly inhibited phenotype transformation, suggesting that the induction of TAM by HA is triggered through binding to CD44. However, besides CD44, other receptors on monocytes can also bind HA. Carlos et al. have reported that CD44 and TLR4 were both engaged in the deactivation of monocytes mediated by HA.¹⁷ Our study cannot exclude other HA receptors in M2 macrophages conversion, which needs a further investigation. Still more, anti-CD44 mAb

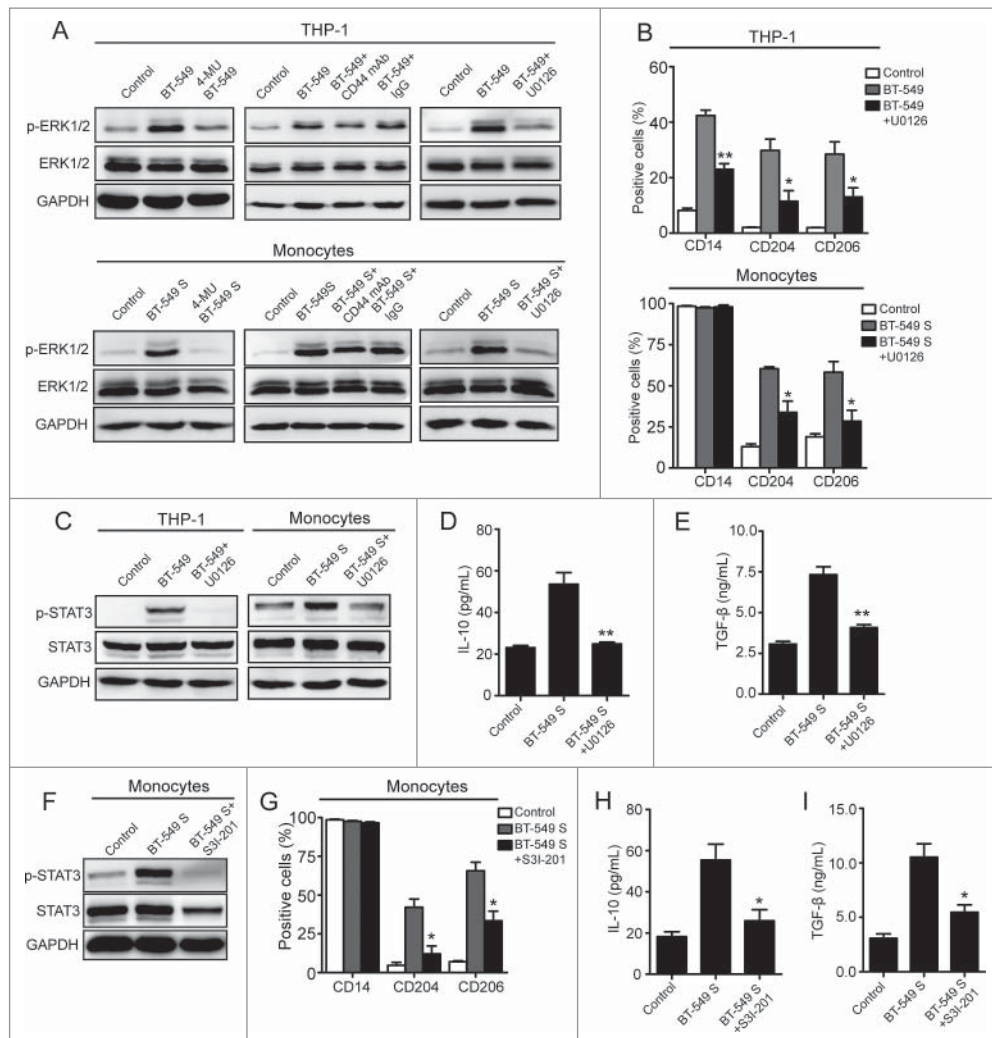


Figure 7. ERK1/2-STAT3 pathway is involved in M2 macrophages formation. (A) Western blot analysis of ERK1/2 phosphorylation levels of THP-1 cells and monocytes. (B, G) Flow cytometry analysis showing expression levels of CD14, CD204, and CD206 in THP-1 cells and monocytes. (C, F) Western blot analysis of STAT3 phosphorylation levels of THP-1 cells and monocytes. (D, E, H, I) Levels of IL-10 and TGF- β secreted by monocytes were measured by ELISA assay. The data represented are shown as mean \pm s.d. collected from three independent experiments. Student's t-tests were performed to assess statistical significance. * $p < 0.05$, ** $p < 0.01$, *** $p < 0.001$ (* VS BT-549 or BT-549S).

or 4-MU cannot completely block the effect of HA on M2 macrophages formation in our experiments, suggesting that additional factors derived from breast cancer cells may participate in the process. Nevertheless, the *in vivo* experiment in mouse model and *in vitro* study, together with the clinical results, still strongly suggest that HA is closely related to M2-like TAM formation within breast tumor microenvironment.

The molecular cues responsible for the change in macrophage phenotypes are mostly unclear. Currently, Simona et al. have reported that c-Jun phosphorylation contributes to the acquisition of a protumorigenic macrophage phenotype in hepatocellular carcinoma,⁴³ implying the importance of signaling pathways in TAM polarization. It is well documented that ERK1/2 signal cascade is closely connected to HA receptor CD44 and has been proved to participate in the regulation of myeloid differentiation and activation.^{44,45} Our data showed that ERK1/2 signal activated by HA-CD44 interaction induced the phenotype transformation of macrophages, implying a novel role of ERK1/2 pathway in macrophages function. It is well known that STAT3 signaling in macrophages is involved in the regulation of immune responses,^{46,47} and STAT3

activation is essential for macrophage differentiation toward the M2 phenotype.²³ In accordance with this, we demonstrated that STAT3 signal was important for monocytes conversion induced by HA derived from breast cancer. Moreover, STAT3 activation was inhibited by suppressing ERK1/2 signal during phenotype transition of macrophages. Our data, together with previous studies indicating that STAT3 may serve as the downstream signal of ERK1/2,^{48,49} suggest that ERK1/2-STAT3 pathway is the molecular cue responsible for HA-mediated TAM formation. Based on these results, we conclude that macrophages within breast tumor microenvironment transform to M2 cells through HA-CD44-ERK1/2-STAT3 pathway that may be valuable as a target in suppressing TAM formation.

In summary, we demonstrate that HA accumulated in breast tumor microenvironment educates recruited monocytes to transform into immunosuppressive TAM through interacting with CD44 and activating the downstream ERK1/2-STAT3 signal pathway. Our study provides a new insight into the mechanisms underlying the formation of M2-like TAM during cancer progress, which would be helpful to breast cancer immunotherapy.

Materials and methods

Patients and specimens

This study was approved by the ethical committee of Shanghai Jiao Tong University Affiliated Sixth People's Hospital, and informed consent was obtained in accordance with the Declaration of Helsinki of the World Medical Association. Patients diagnosed with breast cancer ($n = 42$) or benign breast diseases ($n = 40$) were enrolled into our study. None of the patients had received chemotherapy or radiotherapy before surgery. Details concerning clinical and pathologic parameters are provided in Table 1. Serial slides for immunohistochemistry were obtained from formalin-fixed and paraffin-embedded sections of surgical tumor specimens according to a standard clinical protocol.

Cell lines and preparation of tumor culture supernatants

THP-1, BT-549, and MCF-7 cells were obtained from the American Type Culture Collection (ATCC). All cells were cultured in RPMI1640 supplemented with 10% fetal bovine serum, 100 units/mL penicillin, and 100 $\mu\text{g}/\text{mL}$ streptomycin. BT-549 and MCF-7 cells were plated at 6×10^5 cells in 5 mL complete medium in 60 mm dishes for 24 h, and thereafter changing the medium to new RPMI1640 supplemented with or without 500 $\mu\text{mol}/\text{L}$ 4-MU (4-MU, Sigma, St. Louis, USA), the HA synthesis inhibitor. After three days, the supernatants were harvested, centrifuged, and stored at -80°C .

Immunohistochemistry

Immunohistochemical stainings for HA, CD204, and CD206 were carried out on 5 μm formalin-fixed and paraffin-embedded sections. The serial slides were dewaxed with xylene, and dehydrated through a series of alcohol solutions. After washing in distilled water, the sections were pretreated with citrate buffer for 20 min by a microwave antigen-retrieval procedure. The peroxidase blocking reagent was used to block endogenous peroxidase activity. After washing the slides three times in PBS, non-specific binding was blocked by pre-incubating with 5% bovine serum albumin (BSA) in PBS at room temperature for 1 h. For HA staining, a 1:50 dilution of biotinylated HABP (Merck, Darmstadt, Germany) in 1% BSA-PBS was added, and the slides were incubated at 4°C overnight. Next, slides were washed with PBS and incubated with Streptavidin-ABC at room temperature for 30 min. For CD204/CD206 detection, slides were incubated overnight at 4°C with rabbit anti-human CD204 or CD206 polyclonal antibodies (1:100, Molecular Probes, Eugene, OR, USA). Next, slides were washed with PBS and incubated with biotinylated anti-rabbit antibody (Boster, Wuhan, China) for 30 min at room temperature, followed by incubation with Streptavidin-ABC. Slides were washed and then developed with DAB Substrate Kit and counterstained with hematoxylin. The intensity of HA staining was quantitatively analyzed using Image Pro-Plus 6.0 software (Media Cybernetics, MD, USA). For quantification of CD204- or CD206-positive cells, five randomly selected fields (400 magnifications) were counted and averaged to represent

the numbers of positive cells in the section. Each section was evaluated by two independent investigators who were blind to the patients' clinicopathological data.

Generation of stably transfected cell lines

The HAS2 expression plasmid was generated by cloning the genomic HAS2 gene into retroviral transfer plasmid pCMVIE-IRES-puro to generate plasmid pCMVIE-IRES-HAS2. Briefly, standard PCR was performed to reproduce the HAS2 open reading frame (ORF, Hanbio, Shanghai, China), and the primers used in the reaction included sites for two different restriction enzymes (EcoRI and BamHI, Fermentas, Vilnius, Lithuania). The ORF was inserted into the vector using a standard ligation reaction with T4 DNA Ligase (Fermentas). Amplification of the cloned vector was done via bacterial transformation (*Escherichia coli* DH5 α , Invitrogen, Carlsbad, CA, USA). The integrity of the HAS2 ORF was confirmed by PCR and sequencing. Then, pCMVIE-IRES-HAS2 was cotransfected with pSPAX2 and pMD2Gd in 293T cells. Thirty-six hours after the cotransfection, supernatants were collected and incubated with MCF-7 cells for 24 h in the presence of polybrene (2.5 $\mu\text{g}/\text{mL}$, Santa Cruz, Dallas, USA). After infection, puromycin (1.5 $\mu\text{g}/\text{mL}$, Sigma) was used to select stably transduced cells over a 15-d period. The MCF-7 cells over-expressing HAS2 were named as MCF-7^{HAS2} cells, whereas the MCF-7 cells infected with the control virus were named as MCF-7^{mock} cells. The expression levels of HAS2 and HA in MCF-7^{HAS2} and MCF-7^{mock} cells were determined by western blot and radioimmunoassay, respectively.

Isolation of monocytes and inducement of M2 macrophages formation

Peripheral blood mononuclear cells (PBMC) were isolated from buffy coats derived from the blood of healthy donors by Ficoll density gradient. Cells were initially cultured for 2 h at a density of 1×10^6 cells/mL in RPMI1640 supplemented with antibiotics. Then, the supernatant was removed and adherent cells were cultured in the same medium additionally supplemented with 10% fetal bovine serum for 16 h to remove residual lymphocytes. For inducing the phenotype conversion of macrophages, THP-1 cells were treated with PMA for 6 h and then cultured with PMA plus 20 ng/mL IL-4/IL-13 (eBioscience, San Diego, USA) for additional 18 h, or co-cultured with different breast cancer cells for 72 h. Briefly, breast cancer cells plated at 6×10^5 cells in 25 cm^2 culture flasks were cultured for 24 h, and the culture medium was discarded. The 6×10^5 suspended THP-1 cells in 5 mL RPMI1640 medium were added into the flasks and co-cultured with breast cancer cells for 72 h. Then, THP-1 cells were isolated and prepared for flow cytometry or western blot. For monocytes derived from peripheral blood of healthy donors, 1×10^6 cells were seeded in 25 cm^2 culture flasks and stimulated with IL-4/IL-13 (20 ng/mL) or 50% supernatants from different breast cancer cells for 72 h. Then, monocytes were lysated for immunoblotting analysis or detached by 5 mmol/L EDTA for flow cytometry and cytotoxicity assay. In some experiments, THP-1 cells and monocytes

were pretreated with anti-CD44 mAb, IgG (10 $\mu\text{g}/\text{mL}$, eBioscience), U0126 (10 ng/mL , Cell signaling, Beverly, USA), or S3I-201 (100 $\mu\text{mol}/\text{L}$, Santa Cruz) for 18 h.

Flow cytometric analysis

Cultured cells were harvested and washed with washing buffer (PBS supplemented with 2% BSA, pH 7.4). Cells (1×10^6 cells per sample) were incubated with monoclonal mouse anti-human antibodies CD14-APC (eBioscience), CD204-PE (R&D, Minneapolis, MN, USA), CD206-PE (Biolegend, San Diego, CA, USA), and the relevant isotypes for 30 min at room temperature. Following incubation samples were washed three times and resuspended in PBS. 1×10^4 cells were analyzed per sample on a flow cytometer (Beckman-Coulter, Brea, CA, USA). Gates were determined with the use of appropriate isotype controls. Results were given as the positive percentage minus background from isotype controls.

Western blotting

Cells were harvested and homogenized in ice-cold RIPA lysis buffer. Total cell lysates were collected, and equal quantities of protein were separated by SDS-PAGE and blotted onto PVDF membranes. The PVDF membranes were blocked with Tris-buffered saline (TBS) containing 5% skimmed milk powder for 1 h at room temperature and incubated with anti-phospho-STAT3 (Cell Signaling, 1:1,000), anti-phospho-ERK1/2 (Cell Signaling, 1:1,000) or anti-GAPDH mAb (1:1,000, Abcam, Cambridge, MA, USA) overnight at 4°C. Then the membranes were washed with $1 \times \text{TBS}/\text{Tween}20$ buffer for three times and incubated with HRP-conjugated polyclonal secondary antibodies for 1 h at room temperature. The membranes were developed with the enhanced plus chemiluminescence assay (Millipore, Temecula, CA, USA). Then the membranes for phospho-STAT3 and phospho-ERK1/2 were washed by stripping buffer and blocked for 1 h. After incubated with anti-STAT3 (Cell Signaling, 1:1,000) and anti-ERK1/2 mAb (Cell Signaling, 1:1,000) overnight at 4°C, the membranes were incubated with secondary antibodies and developed with the enhanced plus chemiluminescence assay.

ELISA assay

The IL-10 and TGF- β levels in the conditioned media of monocytes were measured using an enzyme-linked immunosorbent assay (ELISA) kit (eBioscience) according to the manufacturer's instructions. Briefly, a 96-well microplate was precoated with anti-human IL-10 or TGF- β antibody. First, 100 μL of each standard or sample was added to the appropriate wells and incubated for 2.5 h at 24°C with gentle shaking. After discarding the solution and washing four times, 100 μL of prepared biotinylated anti-human IL-10 or TGF- β antibody was added to each well and incubated for 1 h. After washing away unbound biotinylated antibody, 100 μL of horseradish peroxidase (HRP)-conjugated streptavidin was added to the wells and incubated for 45 min, and 100 μL of 3,3',5,5'-Tetramethylbenzidine (TMB) one-step substrate reagent was added after five

washes. Subsequently, 50 μL of stop solution was added to each well, and the plate was immediately read at 450 nm. The endogenous IL-10 and TGF- β production of respective supernatants were simultaneously assayed and minused.

Cytotoxicity assay

Human peripheral blood monocytes (5×10^4 /well) were cultured in normal medium or exposed to BT-549 supernatant for 72 h. Next, monocytes were co-cultured with BT-549 cells which were seeded in 24-well plates (2×10^4 /well) for 24 h. After that, cells were washed briefly with PBS, fixed in 4% paraformaldehyde for 10 min, then permeabilized using Triton X-100 (0.1% v/v in PBS) for 10 min at room temperature. The cells were stained with Hoechst 33342 (Beyotime, Shanghai, China) overnight at 4°C and visualized under an inverted fluorescence microscopy (Olympus, Tokyo, Japan).

Animal experiments

Female NOD/SCID mice were obtained from Shanghai SLAC Laboratory Animal Co. Ltd. All protocols involving mice were evaluated and approved by our Institutional Animal Care and Use Committee and performed under veterinary supervision. MCF-7^{mock} or MCF-7^{HAS2} cells (1×10^7) in a suspension of 50% Matrigel (CorningCostar, Cambridge, USA) were injected into the mammary fat pads of 8-week-old mice. Drinking water of mice was supplemented with 0.67 $\mu\text{g}/\text{mL}$ 17 β -estradiol (Sigma) from one week in advance of inoculation until sacrificed.⁵⁰ Fresh estradiol-supplemented water was provided twice a week. After 30 d, the animals were sacrificed. Tumor samples were isolated, fixed by formalin, and embedded by paraffin for immunohistochemistry.

Statistical analysis

All statistical analyses were carried out using SPSS 16.0 statistical software (SPSS, San Diego, USA). Pearson's correlation was used to test association between continuous variables. Statistical analysis between groups displaying normal distributions was performed by Student's t test for two groups or using one-way ANOVA for multiple groups. When the normality test failed, the analysis was performed using non-parametric tests, such as the Mann-Whitney rank sum test. In all cases, $p < 0.05$ was considered statistically significant.

Disclosure of potential conflicts of interest

No potential conflicts of interest were disclosed.

Funding

This work was supported by the National Natural Science Foundation of China (81272479, 81402419, 81572821, 81502490, 81502491), the Natural Science Foundation of Shanghai Municipality (14YF1412200), the Program of Shanghai Leading Talents (2013-038), the Shanghai Shen-Kang Hospital Development Center (SHDC22014004) and Shanghai Jiao Tong University Affiliated Sixth People's Hospital (1655).

References

- Gordon S, Martinez FO. Alternative activation of macrophages: mechanism and functions. *Immunity* 2010; 32:593-604; PMID:20510870; <http://dx.doi.org/10.1016/j.immuni.2010.05.007>
- Mantovani A, Sozzani S, Locati M, Allavena P, Sica A. Macrophage polarization: tumor-associated macrophages as a paradigm for polarized M2 mononuclear phagocytes. *Trends Immunol* 2002; 23:549-55; PMID:12401408; [http://dx.doi.org/10.1016/S1471-4906\(02\)02302-5](http://dx.doi.org/10.1016/S1471-4906(02)02302-5)
- Chen J, Yao Y, Gong C, Yu F, Su S, Chen J, Liu B, Deng H, Wang F, Lin L et al. CCL18 from Tumor-Associated Macrophages Promotes Breast Cancer Metastasis via PITPNM3. *Cancer Cell* 2011; 19:541-55; PMID:21481794; <http://dx.doi.org/10.1016/j.ccr.2011.02.006>
- Medrek C, Ponten F, Jirstrom K, Leandersson K. The presence of tumor associated macrophages in tumor stroma as a prognostic marker for breast cancer patients. *BMC Cancer* 2012; 12:306; PMID:22824040; <http://dx.doi.org/10.1186/1471-2407-12-306>
- Priceman SJ, Sung JL, Shaposhnik Z, Burton JB, Torres-Collado AX, Moughon DL, Johnson M, Lulis AJ, Cohen DA, Iruela-Arispe ML et al. Targeting distinct tumor-infiltrating myeloid cells by inhibiting CSF-1 receptor: combating tumor evasion of antiangiogenic therapy. *Blood* 2010; 115:1461-71; PMID:20008303; <http://dx.doi.org/10.1182/blood-2009-08-237412>
- Goswami S, Sahai E, Wyckoff JB, Cammer N, Cox D, Pixley FJ, Stanley ER, Segall JE, Condeelis JS. Macrophages promote the invasion of breast carcinoma cells via a colony-stimulating factor-1/epidermal growth factor paracrine loop. *Cancer Res* 2005; 65:5278-83; PMID:15958574; <http://dx.doi.org/10.1158/0008-5472.CAN-04-1853>
- Herr B, Zhou J, Werno C, Menrad H, Namgaladze D, Weigert A, Dehne N, Brüne B. The supernatant of apoptotic cells causes transcriptional activation of hypoxia-inducible factor-1 α in macrophages via sphingosine-1-phosphate and transforming growth factor- β . *Blood* 2009; 114:2140-8; PMID:19549990; <http://dx.doi.org/10.1182/blood-2009-01-201889>
- Weigert A, Schiffmann S, Sekar D, Ley S, Menrad H, Werno C, Grosch S, Geisslinger G, Brüne B. Sphingosine kinase 2 deficient tumor xenografts show impaired growth and fail to polarize macrophages towards an anti-inflammatory phenotype. *Int J Cancer* 2009; 125:2114-21; PMID:19618460; <http://dx.doi.org/10.1002/ijc.24594>
- DeNardo DG, Barreto JB, Andreu P, Vasquez L, Tawfik D, Kolhatkar N, Coussens LM. CD4(+) T cells regulate pulmonary metastasis of mammary carcinomas by enhancing protumor properties of macrophages. *Cancer Cell* 2009; 16:91-102; PMID:19647220; <http://dx.doi.org/10.1016/j.ccr.2009.06.018>
- Banerjee S, Lin C-FL, Skinner KA, Schiffhauer LM, Peacock J, Hicks DG, Redmond EM, Morrow D, Huston A, Shayne M et al. Heat shock protein 27 differentiates tolerogenic macrophages that may support human breast cancer progression. *Cancer Res* 2011; 71:318-27; PMID:21224361; <http://dx.doi.org/10.1158/0008-5472.CAN-10-1778>
- Toole BP. Hyaluronan: from extracellular glue to pericellular cue. *Nat Rev Cancer* 2004; 4:528-39; PMID:15229478; <http://dx.doi.org/10.1038/nrc1391>
- Auvinen P, Tammi R, Parkkinen J, Tammi M, Agren U, Johansson R, Hirvikoski P, Eskelinen M, Kosma VM. Hyaluronan in peritumoral stroma and malignant cells associates with breast cancer spreading and predicts survival. *Am J Pathol* 2000; 156:529-36; PMID:10666382; [http://dx.doi.org/10.1016/S0002-9440\(10\)64757-8](http://dx.doi.org/10.1016/S0002-9440(10)64757-8)
- Tammi RH, Kultti A, Kosma V-M, Pirinen R, Auvinen P, Tammi MI. Hyaluronan in human tumors: Pathobiological and prognostic messages from cell-associated and stromal hyaluronan. *Semin Cancer Biol* 2008; 18:288-95; PMID:18468453; <http://dx.doi.org/10.1016/j.semcancer.2008.03.005>
- Jiang DH, Liang JR, Fan J, Yu S, Chen SP, Luo Y, Prestwich GD, Mascarenhas MM, Garg HG, Quinn DA et al. Regulation of lung injury and repair by toll-like receptors and hyaluronan. *Nat Med* 2005; 11:1173-9; PMID:16244651; <http://dx.doi.org/10.1038/nm1315>
- Duff MD, Mestre J, Maddali S, Yan ZP, Stapleton P, Daly JM. Analysis of gene expression in the tumor-associated macrophage. *J Surg Res* 2007; 142:119-28; PMID:17597158; <http://dx.doi.org/10.1016/j.jss.2006.12.542>
- Mytar B, Woloszyn M, Szatanek R, Baj-Krzyworzeka M, Siedlar M, Ruggiero I, Wieckiewicz J, Zembala M. Tumor cell-induced deactivation of human monocytes. *J Leukoc Biol* 2003; 74:1094-101; PMID:12960282; <http://dx.doi.org/10.1189/jlb.0403140>
- del Fresno C, Otero K, Gomez-Garcia L, Gonzalez-Leon MC, Soler-Ranger L, Fuentes-Prior P, Escoll P, Baos R, Caveda L, Garcia F et al. Tumor cells deactivate human monocytes by up-regulating IL-1 receptor associated kinase-M expression via CD44 and TLR4. *J Immunol* 2005; 174:3032-40; PMID:15728517; <http://dx.doi.org/10.4049/jimmunol.174.5.3032>
- Bourcier S, Sansonetti A, Durand L, Chomienne C, Robert-Lezennes J, Smadja-Joffe F. CD44-ligation induces, through ERK1/2 pathway, synthesis of cytokines TNF- α and IL-6 required for differentiation of THP-1 monoclonal leukemia cells. *Leukemia* 2010; 24:1372-5; PMID:20508620; <http://dx.doi.org/10.1038/leu.2010.100>
- Zhang G, Zhang H, Liu Y, He Y, Wang W, Du Y, Yang C, Gao F. CD44 clustering is involved in monocyte differentiation. *Acta Bioch Bioph Sin* 2014; 46:540-7; <http://dx.doi.org/10.1093/abbs/gmu042>
- Tsuchiya S, Kobayashi Y, Goto Y, Okumura H, Nakae S, Konno T, Tada K. Induction of maturation in cultured human monocytic leukemia cells by a phorbol diester. *Cancer Res* 1982; 42:1530-6; PMID:6949641
- Komohara Y, Ohnishi K, Kuratsu J, Takeya M. Possible involvement of the M2 anti-inflammatory macrophage phenotype in growth of human gliomas. *J Pathol* 2008; 216:15-24; PMID:18553315; <http://dx.doi.org/10.1002/path.2370>
- Larsson K, Kock A, Idborg H, Henriksson MA, Martinsson T, Johnsen JI, Korotkova M, Kogner P, Jakobsson PJ. COX/mPGES-1/PGE(2) pathway depicts an inflammatory-dependent high-risk neuroblastoma subset. *Proc Natl Acad Sci USA* 2015; 112:8070-5; PMID:26080408; <http://dx.doi.org/10.1073/pnas.1424355112>
- Sica A, Bronte V. Altered macrophage differentiation and immune dysfunction in tumor development. *J Clin Invest* 2007; 117:1155-66; PMID:17476345; <http://dx.doi.org/10.1172/JCI31422>
- Kuang D-M, Wu Y, Chen N, Cheng J, Zhuang S-M, Zheng L. Tumor-derived hyaluronan induces formation of immunosuppressive macrophages through transient early activation of monocytes. *Blood* 2007; 110:587-95; PMID:17395778; <http://dx.doi.org/10.1182/blood-2007-01-068031>
- Mosser DM, Zhang X. Interleukin-10: new perspectives on an old cytokine. *Immunol Rev* 2008; 226:205-18; PMID:19161426; <http://dx.doi.org/10.1111/j.1600-065X.2008.00706.x>
- Bierie B, Moses HL. Transforming growth factor β (TGF- β) and inflammation in cancer. *Cytokine Growth Factor Rev* 2010; 21:49-59; PMID:20018551; <http://dx.doi.org/10.1016/j.cytogfr.2009.11.008>
- Kim HR, Wheeler MA, Wilson CM, Iida J, Eng D, Simpson MA, McCarthy JB, Bullard KM. Hyaluronan facilitates invasion of colon carcinoma cells in vitro via interaction with CD44. *Cancer Res* 2004; 64:4569-76; PMID:15231668; <http://dx.doi.org/10.1158/0008-5472.CAN-04-0202>
- Bourguignon LYW, Gilad E, Rothman K, Peyrollier K. Hyaluronan-CD44 interaction with IQGAP1 promotes Cdc42 and ERK signaling, leading to actin binding, Elk-1/estrogen receptor transcriptional activation, and ovarian cancer progression. *J Biol Chem* 2005; 280:11961-72; PMID:15655247; <http://dx.doi.org/10.1074/jbc.M411985200>
- Yang C, Cao M, Liu H, He Y, Xu J, Du Y, Liu Y, Wang W, Cui L, Hu J et al. The high and low molecular weight forms of hyaluronan have distinct effects on CD44 clustering. *J Biol Chem* 2012; 287:43094-107; PMID:23118219; <http://dx.doi.org/10.1074/jbc.M112.349209>
- Barbieri I, Pensa S, Pannellini T, Quaglino E, Maritano D, Demaria M, Voster A, Turkson J, Cavallo F, Watson CJ et al. Constitutively active stat3 enhances neu-mediated migration and metastasis in mammary tumors via upregulation of cten. *Cancer Res* 2010; 70:2558-67; PMID:20215508; <http://dx.doi.org/10.1158/0008-5472.CAN-09-2840>
- Siddiquee K, Zhang S, Guida WC, Blaskovich MA, Greedy B, Lawrence HR, Yip ML, Jove R, McLaughlin MM, Lawrence NJ et al. Selective chemical probe inhibitor of Stat3, identified through structure-based virtual screening, induces antitumor activity. *Proc Natl Acad Sci*

- Sci USA 2007; 104:7391-6; PMID:17463090; <http://dx.doi.org/10.1073/pnas.0609757104>
32. Iijima J, Konno K, Itano N. Inflammatory alterations of the extracellular matrix in the tumor microenvironment. *Cancer* 2011; 3:3189-205; PMID:24212952; <http://dx.doi.org/10.3390/cancers3033189>.
 33. Tiainen S, Tumelius R, Rilla K, Hamalainen K, Tammi M, Tammi R, Kosma VM, Oikari S, Auvinen P. High numbers of macrophages, especially M2-like (CD163-positive), correlate with hyaluronan accumulation and poor outcome in breast cancer. *Histopathology* 2015; 66:873-83; PMID:25387851; <http://dx.doi.org/10.1111/his.12607>
 34. Kobayashi N, Miyoshi S, Mikami T, Koyama H, Kitazawa M, Takeoka M, Sano K, Amano J, Isogai Z, Niida S et al. Hyaluronan deficiency in tumor stroma impairs macrophage trafficking and tumor neovascularization. *Cancer Res* 2010; 70:7073-83; PMID:20823158; <http://dx.doi.org/10.1158/0008-5472.CAN-09-4687>
 35. Ye XZ, Xu SL, Xin YH, Yu SC, Ping YF, Chen L, Xiao HL, Wang B, Yi L, Wang QL et al. Tumor-associated microglia/macrophages enhance the invasion of glioma stem-like cells via TGF- β 1 signaling pathway. *J Immunol* 2012; 189:444-53; PMID:22664874; <http://dx.doi.org/10.4049/jimmunol.1103248>
 36. Vigetti D, Rizzi M, Viola M, Karousou E, Genasetti A, Clerici M, Bartolini B, Hascall VC, De Luca G, Passi A. The effects of 4-methylumbelliferone on hyaluronan synthesis, MMP2 activity, proliferation, and motility of human aortic smooth muscle cells. *Glycobiology* 2009; 19:537-46; PMID:19240269; <http://dx.doi.org/10.1093/glycob/cwp022>
 37. Clarkin CE, Allen S, Wheeler-Jones CP, Bastow ER, Pitsillides AA. Reduced chondrogenic matrix accumulation by 4-methylumbelliferone reveals the potential for selective targeting of UDP-glucose dehydrogenase. *Matrix Biol* 2011; 30:163-8; PMID:21292001; <http://dx.doi.org/10.1016/j.matbio.2011.01.002>
 38. Funahashi M, Nakamura T, Kakizaki I, Mizunuma H, Endo M. Stimulation of small proteoglycan synthesis by the hyaluronan synthesis inhibitor 4-Methylumbelliferone in human skin fibroblasts. *Connect Tissue Res* 2009; 50:194-202; PMID:19444760; <http://dx.doi.org/10.1080/03008200802684615>
 39. Okuda H, Kobayashi A, Xia B, Watabe M, Pai SK, Hirota S, Xing F, Liu W, Pandey PR, Fukuda K et al. Hyaluronan synthase HAS2 promotes tumor progression in bone by stimulating the interaction of breast cancer stem-like cells with macrophages and stromal cells. *Cancer Res* 2012; 72:537-47; PMID:22113945; <http://dx.doi.org/10.1158/0008-5472.CAN-11-1678>
 40. Saito T, Dai T, Asano R. The hyaluronan synthesis inhibitor 4-methylumbelliferone exhibits antitumor effects against mesenchymal-like canine mammary tumor cells. *Oncol Lett* 2013; 5:1068-74; PMID:23426189; <http://dx.doi.org/10.3892/ol.2013.1124>
 41. Lee JH, Lee GT, Woo SH, Ha YS, Kwon SJ, Kim WJ, Kim IY. BMP-6 in renal cell carcinoma promotes tumor proliferation through IL-10-dependent M2 polarization of tumor-associated macrophages. *Cancer Res* 2013; 73:3604-14; PMID:23633487; <http://dx.doi.org/10.1158/0008-5472.CAN-12-4563>
 42. Jiang D, Liang J, Noble PW. Hyaluronan as an immune regulator in human diseases. *Physiol Rev* 2011; 91:221-64; PMID:21248167; <http://dx.doi.org/10.1152/physrev.00052.2009>
 43. Hefetz-Sela S, Stein I, Klieger Y, Porat R, Sade-Feldman M, Zreik F, Nagler A, Pappo O, Quagliata L, Dazert E et al. Acquisition of an immunosuppressive protumorigenic macrophage phenotype depending on c-Jun phosphorylation. *Proc Natl Acad Sci USA* 2014; 111:17582-7; PMID:25422452; <http://dx.doi.org/10.1073/pnas.1409700111>
 44. Carter AB, Monick MM, Hunninghake GW. Both Erk and p38 kinases are necessary for cytokine gene transcription. *Am J Respir Cell Mol Biol* 1999; 20:751-8; PMID:10101008; <http://dx.doi.org/10.1165/ajrcmb.20.4.3420>
 45. Miranda MB, Johnson DE. Signal transduction pathways that contribute to myeloid differentiation. *Leukemia* 2007; 21:1363-77; PMID:17443228; <http://dx.doi.org/10.1038/sj.leu.2404690>
 46. Matsukawa A, Takeda K, Kudo S, Maeda T, Kagayama M, Akira S. Aberrant inflammation and lethality to septic peritonitis in mice lacking STAT3 in macrophages and neutrophils. *J Immunol* 2003; 171:6198-205; PMID:14634136; <http://dx.doi.org/10.4049/jimmunol.171.11.6198>
 47. Takeda K, Clausen BE, Kaisho T, Tsujimura T, Terada N, Forster I, Akira S. Enhanced Th1 activity and development of chronic enterocolitis in mice devoid of Stat3 in macrophages and neutrophils. *Immunity* 1999; 10:39-49; PMID:10023769; [http://dx.doi.org/10.1016/S1074-7613\(00\)80005-9](http://dx.doi.org/10.1016/S1074-7613(00)80005-9)
 48. Lyu JH, Huang B, Park D-W, Baek S-H. Regulation of PHLDA1 Expression by JAK2-ERK1/2-STAT3 Signaling Pathway. *J Cell Biochem* 2016; 117:483-90; PMID:26239656; <http://dx.doi.org/10.1002/jcb.25296>
 49. Lin W-F, Chen C-J, Chang Y-J, Chen S-L, Chiu I-M, Chen L. SH2B1 β enhances fibroblast growth factor 1 (FGF1)-induced neurite outgrowth through MEK-ERK1/2-STAT3-Egr1 pathway. *Cell Signal* 2009; 21:1060-72; PMID:19249349; <http://dx.doi.org/10.1016/j.cellsig.2009.02.009>
 50. Kim J, Villadsen R, Sorlie T, Fogh L, Gronlund SZ, Fridriksdottir AJ, Kuhn I, Rank F, Wielenga VT, Solvang H et al. Tumor initiating but differentiated luminal-like breast cancer cells are highly invasive in the absence of basal-like activity. *Proc Natl Acad Sci USA* 2012; 109:6124-9; PMID:22454501; <http://dx.doi.org/10.1073/pnas.1203203109>